Journal of the Korean Crystal Growth and Crystal Technology
Vol. 13, No. 1 (2003) 5-14

Stability of the growth process at pulling large alkali halide single crystals

V.I. Goriletsky†, S.K. Bondarenko, M.M. Smirnov, V.I. Sumin, K.V. Shakhova, V.S. Suzdal and V.A. Kuznetzov

Scientific-Research Department of Alkali Halide Crystals STC «Institute for Single Crystals» NAS of Ukraine, Kharkov, Ukraine

(Received August 29, 2002)
(Accepted December 6, 2002)

Abstract Principles of a novel pulse growing method are described. The method realized in the crystal growing on a seed from melts under raw melt feeding provided a more reliable control of the crystallization process when producing large alkali halide crystals. The slow natural convection of the melt in the crucible at a constant melt level is intensified by rotating the crucible, while the crystal rotation favors a more symmetrical distribution of thermal stresses over the crystal cross-section. Optimum rotation parameters for the crucible and crystal have been determined. The spatial position of the solid/liquid phase interface relatively to the melt surface, heaters and the crucible elements are considered. Basing on that consideration, a novel criterion is stated, that is, the immersion extent of the crystallization front (CF) convex toward the melt. When the crystal grows at a «negative» CF immersion, the raised CF may tear off from the melt partially or completely due to its weight. This results in avoid formation in the crystal. Experimental data on the radial crystal growth speed are discussed. This speed defines the formation of a gas phase layer at the crystal surface. The layer thickness is a function of time a temperature at specific values of pressure in the furnace and the free melt surface dimensions in the gap between the crystal and crucible wall. Analytical expressions have been derived for the impurity component mass transfer at the steady-state growth stage describing two independent processes, the impurity mass transfer along the «feed-melt-crystal» path and its transit along the *«feed-melt-gas phase-cold furnace wall»* one. The heater (and thus the melt) temperature variation is inherent in any control system. It has been shown that when random temperature changes occur causing its lowering at a rate exceeding 0.5°C/min, a kind of the CF decoration by foreign impurities or by gas bubbles takes place. Short-term temperature changes at one heater or both result in local (i.e., at the front) redistribution of the preset axial growth speed.

Key words Crystal growth, Process control, Mass transfer, Crystallization front, Gas phase

1. Introduction

It is known from the practice of single crystal production at continuous pulling and continuous process control [1] that the non-uniformity of the crystal cross-section is due to variations in the crystallization front (CF) shape, increase of the crystal part immersed in the melt as its length rises, and time instabilities in the melt feeding by raw material. The above factors were avoided by using a technique providing a pulsed crystal pulling with time-discrete measuring of the melt level relatively to its constant value [2]. The technique provides a high sensitivity and independence of the crystal diameter measurements of the crystallization conditions and makes it possible to obtain a stable diameter over the whole crystal length (up to 700 mm) independent of any FC shape fluctuations, feed rate, parasite crystallization at the crucible walls, etc. This problem has been solved successfully for CsI (Na) scintillation single crystals where the matrix and activator vapor pressure values are similar to each other [3, 4]. In production of large CsI (Tl) or NaI (Tl) single crystals, technical difficulties arise due to that the activator evaporation rate exceeds that of the matrix material. A specific feature of this process is defined by that the melt volume change due to pulling of the crystal immersed therein manifests itself only within the gap between the crucible and crystal and is defined by the area ratio of the CF to the free melt surface (F_L) in that gap [5]. This circumstance poses more strict requirements to some technologic parameters of the growing process. In this connection, the control means of novel generation has been developed to grow single crystals of diameter (d) over 500 mm in reproducible manner, at the diameter deviation from the preset value ($\Delta d/d$) no more than 1.5 % and homogeneous activator distribution over the crystal volume.

†Corresponding author
Tel: +380-0572-307906
Fax: +380-0572-321082
E-mail: vig@isc.kharkov.com

2. Discussion

The work was done using "ROST" type units. The

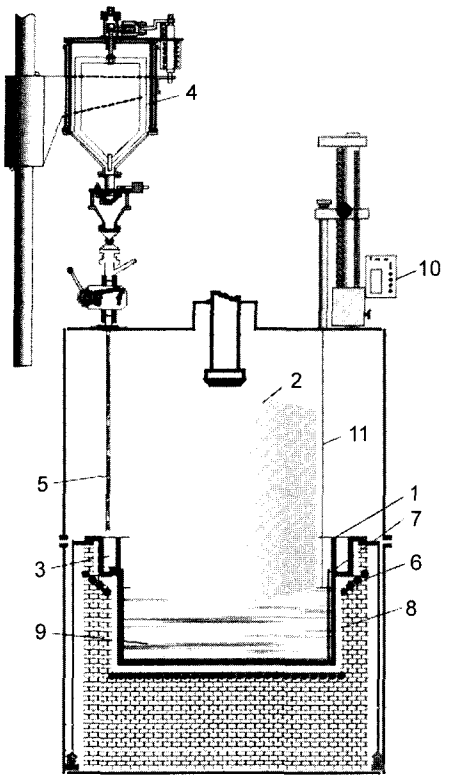

Fig. 1. Growth furnace of the «ROST» unit. 1-platinum crucible; 2-crystal; 3-peripheral circular vessel; 4-hopper with feeder; 5-transport tube; 6-side heater; 7-holes; 8-crucible screen; 9-melt; 10-melt level sensor; 11-melt level sensor probe.

vacuum furnace is provided with crucibles of 500 or 600 mm in diameter where a constant melt level is maintained. The continuous melt feeding by raw material is provided alternately from two changeable vacuum hoppers with feeders connected with the vacuum furnace via a lock system. It is seen from the scheme presented in Fig. 1 that to compensate the melt level lowering in the crucible (1) during the crystal (2) growth, a circular peripheral vessel (3) is provided receiving the raw material from the hopper and feeder (4) via the transport tube (5). After the salt is melted by the side heater (6), the melt flows through holes (7) into the space defined by the crucible wall and screen (8) and then mixes with the melt (9), the level of the latter being measured using a heated probe (11) of the melt level sensor (10). The independent peripheral vessel (3) of the crucible 1 has an independent so-called side heater (6). When the salt is melted in controlled manner within the vessel (3), the melt degassing occurs simultaneously, thus making it possible to obtain crystals free of gas inclusions.

2.1. *The growth process control*

The novel generation of control means is represented by the three-level digital system [6]. The first level is an analog one and includes the bottom heater temperature controller, the melt level measuring device, the crystal holder rod displacing means and the melt feeding device. The second level includes microprocessor controllers of the crystal pulling and heater temperature as well as analog-digital converter; these devices provide the data collection and processing for transmission to the uppermost third level of the system. The latter consists of an AT 486 DX PC with various peripheral devices. Such a system provides a more efficient control by an additional signal differentiation, comparison of the result obtained with a mathematical model of the melt level change speed and generation of an additional correcting commands during intervals between feeding cycles.

Unfortunately, even such a precise control of large single crystal growth process does not exclude completely any malfunctions resulting in temperature jumps at one of the heaters or the cooling water temperature and pressure changes in the outer furnace jacket.

In what follows, the study results are presented being a basis for an attempt to determine the critical values of most important crystallization parameters defining the stability of large single crystal growth process.

2.2. *Crucible and crystal rotation parameters*

The features inherent in the crystal growing on a seed are intended to eliminate the defects of the Stockbarger methods where ampoules are used. So, both crucible and crystal rotation in growth units favors a more homogeneous temperature distribution in the melt and the crystal that is a factor of importance when large cross-section crystals are grown. The slow convection of the melt is enhanced by the crucible (and thus the melt) rotation while the crystal rotation favors a more symmetric distribution of thermal stresses over the crystal cross-section. The crystal diameter increase requires an appropriate correction of the process parameters. When selecting the crucible and crystal rotation parameters, the ration of the crucible diameter, D, to the melt height (H) therein is decisive. At $D/H \leq 3$, the crucible and crystal rotation in opposite directions at speeds of 0.5 to 2 revolutions per minute is used successfully; but at $D/H > 3$, this procedure is impermissible even at low speeds, since it results in turbulent flows in the melt causing loss of the FC surface smoothness.

The primary condition defining the crucible rotation frequency is the requirement of complete salt melting in the peripheral circular vessel of the crucible at the side

heater temperature (T_{side}) exceeding the salt melting point by 10 to 20°C (the T_{side} parameter is determined in experiment and depends on the axial temperature gradient in the furnace). The crucible rotation speed is thus associated strongly with the T_{side} that can be varied within a narrow range only as well as with constant geometric dimensions of the circular peripheral vessel (where the salt is spread over). Its experimental values lie within narrow limits of 0.8 to 1.5 min^{-1}.

When growing crystals of over 500 mm diameter from a crucible with a constant melt level of 100 to 125 mm, i.e., the $D/H \approx 5$, another approach is necessary to provide the stable growth. The considerable CF surface area of a large crystal contributes more efficiently to the melt mixing, therefore, the crystal and crucible rotation in opposite directions result in an intricate flow pattern in the melt causing the loss of the CF smoothness (Fig. 2).

Reproducible results as to the CF stability were obtained at the crystal and crucible rotation in the same direction at the crystal rotation frequency of 1 to 2 min^{-1} but at the crucible rotation frequency delay by 5 to 10 % when rotating clockwise or at the crystal rotation frequency delay by 5 to 10 % when rotating counterclockwise. The difference in rotation frequencies is explained by that it is necessary to exclude the spontaneous crystal screwing-off together with the captive nut of the crystal rod under its slight vibration or due to the crystal weight. Such a range of the rotation frequency does not result in any side effects on the laminar melt flow structure and thus favors the stable crystal growth.

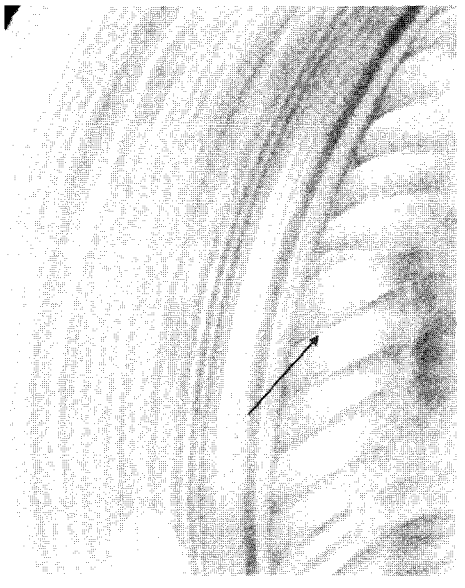

Fig. 2. Growth process disturbance manifested as the crystallization front shape smoothness loss at NaI (Tl) crystal of 500 mm dia. (shown by arrow) growing at the rotation speed 4 min^{-1}.

2.3. *Limiting diameter of crystal in growth*

The temperature field character in the melt defining convective flows therein (involved, in turn, in formation of isothermal solid/liquid interface) is defined also by the crystal diameter (d) ratio to the crucible one (D). At $d/D = 0.8$ the formed front is convex while it is substantially flat at $d/D = 0.5$ and includes a considerable part of the melt volume at $d/D = 0.9$.

Many years of experience in growing single crystals by semi-continuous technique using «ROST» units have proved that it is just d/D value of 0.83 that is the limiting ratio. At a higher ratio, the CF shape tends to intricate variations consisting in that the immersed part diameter exceeds that of the crystal above the growth surface.

2.4. *The crystallization front immersion depth relative to the melt surface*

A substantial specific feature of the Kyropoulos technique (the method under consideration being a modification thereof) is the spatial arrangement of the interface with respect to the melt surface, the crucible elements and heaters when crystals of different diameters are grown. If the preset crystal diameter does not exceed 30 mm, the CF is above the melt surface (similar to the

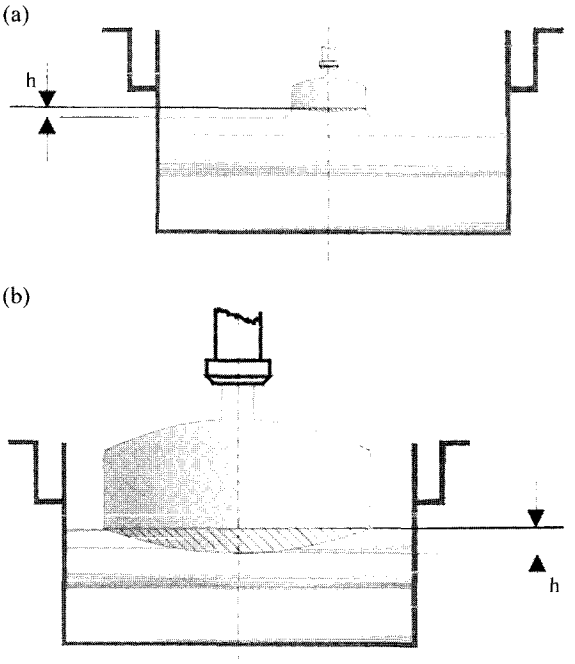

Fig. 3. Superposition scheme of spatial arrangement of crystallization fronts relative to the melt surface for growing crystals of up to 30 mm (a) and about 500 mm (b).

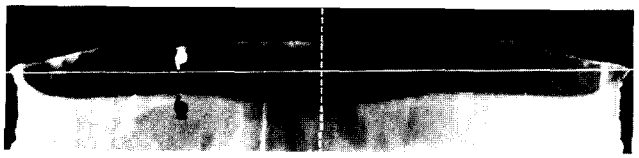

Fig. 4. Longitudinal section of the crystallization front of a 500 mm dia. NaI (Tl) single crystal with two «maxima» being 18 mm from the melt table (the immersion value is pointed by indicating signs).

Czochralski technique), that is, the melt is a certain distance +h lifted by the growing crystal front (Fig. 3a) while at the crystal diameter over 30 mm, the front should be shifted towards the crucible bottom with respect to the melt surface (Fig. 3b) in order to provide the stable growth. In other words, the CF should be immersed into the melt to some distance –h, a uniform CF curvature being formed. In practice, however, such situation is rather desirable than attainable spontaneously.

The problem of the CF uniform convexity towards the melt is particularly critical when crystals of more than 300 mm diameter are to be grown. Figures 4 and 5 present two types of the most often occurring biconvex CF (in longitudinal crystal section, the CF has two «maxima» at the middle part of radius and three «minima», two at periphery and one in center) with different immersion depths into melt that is seen from their distances to the white line answering to the free melt surface position. (The «extreme» points were determined graphically). Let the term «CF immersion depth» mean the minimum distance from the free melt surface to «maxima» (at the biconvex CF shape in section), if present, or to «minimum» (at the uniformly convex shape). The case shown in Fig. 4 where the average immersion depth of CF points nearest to the free melt surface is about 18 mm occurs most often in the upper crystal part only and then it passes to the uniformly convex shape as the cylindrical part length increases. The admissible CF immersion depth under the melt surface is 10 mm. At

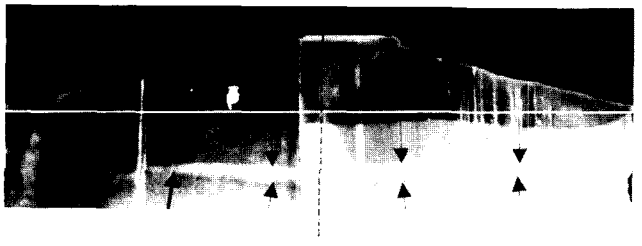

Fig. 5. Longitudinal section of the crystallization front of a 500 mm dia. NaI (Tl) single crystal with two «maxima» being 7 mm from the melt surface (the immersion value is pointed by indicating signs.

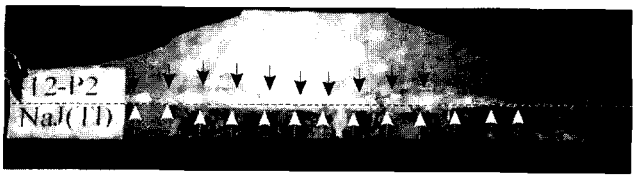

Fig. 6. An example of the crystallization front «negative» immersion (the front is above the melt surface) at growing of NaI (Tl) crystal of 520 mm in dia. The black dashed horizontal line answers to the free melt surface level. The black arrows indicate the upper boundary of the formed void (the crystallization front trace); the white ones, the upper boundary of the crystal part different from the seed in crystallographic orientation.

smaller immersion depth, the CF is the origin of structure defects and a runoff for foreign impurities. This is seen in the central part of Fig. 5 where the CF immersion depth is 7 mm. A further diminution of the CF immersion depth results in more complex and undesirable disturbances in the growth process.

For example, if a large crystal is grown at a «negative» immersion depth of CF maxima and even its minima (Fig. 6), the melt can be torn off from the CF resulting in formation of a void at the phase interface. Such a void can spread over a considerable part of the crystal cross-section (after the void was formed, the growing crystal was borne by the peripheral ring of the basis orientation [001] set by the seed). As is seen in

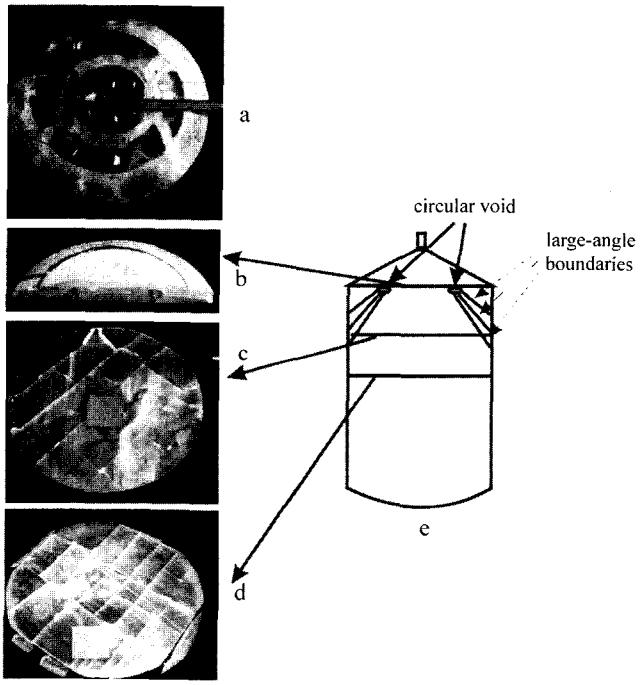

Fig. 7. Formation of a circular void in the upper part of a NaI (Tl) single crystal. a- the crystal cross-section above the void; b, c, d- the longitudinal section in the crystal center, e-scheme formation of a circular void and large-angle.

Fig. 5, the void arch in the crystal was coated with the deposit formed from the melt vapor phase and after a certain time the void itself was crystallized in an arbitrary orientation under formation of large-angle boundaries. A particular case of situation shown in Fig. 6 is a local melt tear-off from the CF under formation of a circular bubble (see Fig. 7). This occurs just in the CF sites raised maximally above the free melt surface and is possible only in the case of biconvex or convex CF. In spite of these complications, the growing process may be continued as a rule and, as is seen in Figs. 7b and 7d, an ingot of about 400 kg mass may be obtained having the single crystal structure in the predominant fraction of its volume and retaining the integrity after cooling.

At the crystal growth speed of 2 to 4 mm/h, the biconvex interface shape is stable against external factors (mainly the controlled and random temperature fluctuations), bubble formation and local activator distribution inhomogeneities in the crystal volume, if the CF immersion depth is at least 10 mm. Already at the crystal cylindrical part length (L) about 60 mm, such CF shape is transformed very slowly into an uniform convex one, the h value being increased towards the lower part. The h(L) dependence is essentially linear for d = 520 mm while being more complex for d = 440 mm. This distinction in the h(L) curve character is due mainly by difference in the crucible diameter ratio to the furnace one that defines the heat losses from the crucible surface and thus from the total side surface of the crystal.

The axial temperature gradient in the furnace defines the h(L) change extent as the crystal length increases, other parameter being constant. A slight temperature gradient in the growth furnace (about 10 deg/cm) provides the smoothness of inevitable h(L) variations. Both phenomena are typical of ROST units. This is confirmed by data on the actual CF sag values in the grown crystals [7].

Although there are no experimental data pointing explicitly to drawbacks of biconvex CF shape, it is just convex CF that is to be tried to attain in practice.

2.4. *Formation of convex crystallization front*

In the method under consideration, the CF shape is defined by relation between contributions of both heaters (side and bottom ones) to the total temperature field and by configuration of convective flows in the melt. In the simplest case, the use of a typical heater with uniform Archimedes spiral (equidistant winding) results in above-mentioned CF shapes (dual change of the CF curvature sign). This is associated in first turn with large cross-section peculiarities, as well as with the seed cooling, specific features of the melted salt transportation from the peripheral circular vessel to the main crucible part, etc.

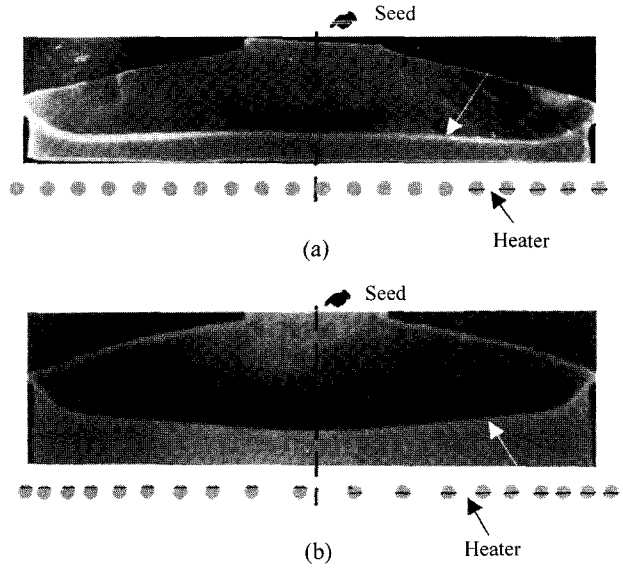

Fig. 8. Change (shown by arrow) of crystallization front shape revealed in longitudinal sections of upper parts of NaI (Tl) single crystals of 440 mm dia. a- Initial CF shape at uniform distribution of the bottom heater power (the heater is shown schematically under the crystal photo). b- CF shape after radial redistribution of the heater power (power reduction in the central part and increase in the peripheral one by varying winding spacing.

The convective flows cause in this case formation of biconvex or concave CF (Fig. 8a) differing in their parameters; this can be seen in longitudinal sections of upper parts of doped crystals. (Since the crystal is grown up to the preset diameter in the absence of activator that is introduced into the melt according to predetermined program only after the longitudinal growth process is initiated, the boundary between undoped and doped crystal parts can be visualized by UV excitation in the upper part longitudinal section). The radial distribution of the bottom heater power is a factor of importance defining the CF shape and convective flow formation. Under account for the specific features of temperature field caused by the heater arrangement geometry, the uniform radial distribution of the bottom heater power results in a non-uniform heating of the crucible bottom where the thermal flux decreases towards its periphery. In designing, a preset smooth non-uniformity of the radial heat flux from the bottom heater is to be provided (decreasing heat flow from periphery to center). This is realized by experimental trials.

This experimental fact, contradictory at a first glance, is a result of the total heat transfer process along the "*heater-crucible and melt-crystal-cooled crystal holder and its environment*" sequence under account for all heat transfer mechanisms.

2.5. *Crystal radial growth speed*

As mentioned above, the bottom temperature (T_{bot}) has a minimum at the longitudinal growth stage (T_{bot} min) answering to the moment when the upper crystal butt crosses the crucible upper edge. Then, T_{bot} (and thus the melt temperature) starts to increase (Fig. 12). This is the most crucial moment in the crystal growing, since the position of T_{bot} min changes from one run to another and depends on numerous parameters such as the crystal final diameter, pressure within the furnace, the melt color, cooling intensity of the crystal holder rod and furnace, as well as on the growth process dynamics. Figure 9 presents a large CsI (Tl) crystal of 450 mm in diameter with longitudinal section in foreground where it is seen that, at the cylindrical crystal part height about 55 mm (it is just that height where T_{bot} min was observed), a distortion in the crystallization process occurred resulting in an impurity phase inclusion (seen as a cloud). In spite of short duration of this event followed by temperature elevation, the central part of this crystal is unsuitable for manufacturing of large scintillation modules.

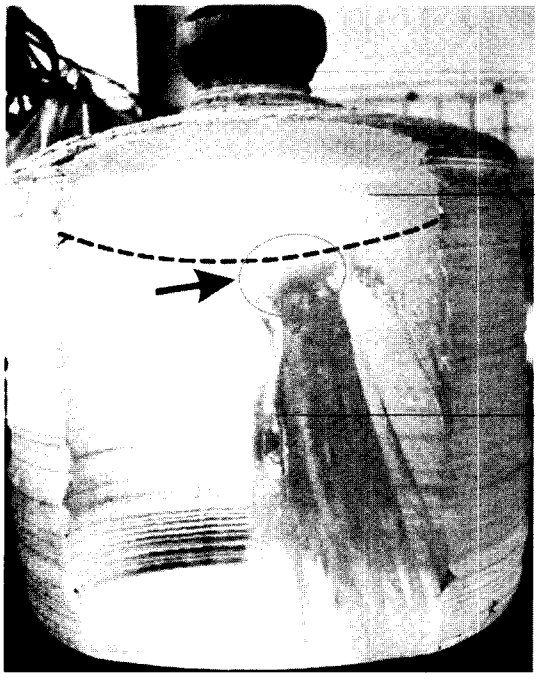

Fig. 9. Formation of polycrystal nuclei (shown by arrow) at the CF center in growing CsI (Tl) crystal of 450 mm dia. The CF shape in shown by dashed line.

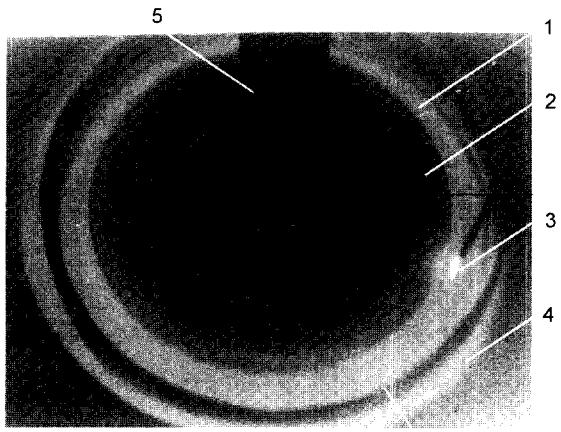

Fig. 10. Top butt view of a NaI (Tl) single crystal of 520 mm dia. in growing. The photo has been taken in IR light through the upper eye glass of the «ROST» unit. 1- the free melt surface; 2- the crystal butt; 3- the melt level sensor probe; 4- circular peripheral vessel of the crucible; 5- the crystal holder rod; 6- vertical wall of the circular peripheral vessel.

The natural melt evaporation that can be controlled within limits of permissible pressure in the furnace causes a deposit formation from gas phase at the crystal surface and the furnace walls, the deposit layer thickness being defined mainly by the crystal radial growth speed. The gas phase deposition rate, and thus the deposit thickness, is a function of time and temperature at specific values of pressure in the furnace and the gap dimensions (F_L) between the crystal and crucible. As the crystal diameter increases, the F_L becomes smaller (the growing crystal overlaps the melt surface where not only evaporation occurs but also heat loss to the environment). A photo (Fig. 10) taken directly in the course of crystal growth at the initial steady stage without any additional illumination in the furnace illustrates the temperature difference (seen as the color one) between the crystal butts and melt. The denser and thicker is the deposit layer on the crystal, the darker is the crystal upper butt, the less is heat release from the crystal to environment and the lower is T_{bot} min in the crucial process moment. The primary factors defining the melt temperature at this stage are the crystal surface transmittance to its intrinsic IR radiation and the heat conductivity of the crystallization front convex toward the melt on the furnace inner walls. It follows from visual observations of the crystal butt color at the transition moment from the radial crystal growth to longitudinal one and of the T_{bot} min position that there is a direct relationship: the lighter is the crystal butt, the higher is T_{bot} min. In

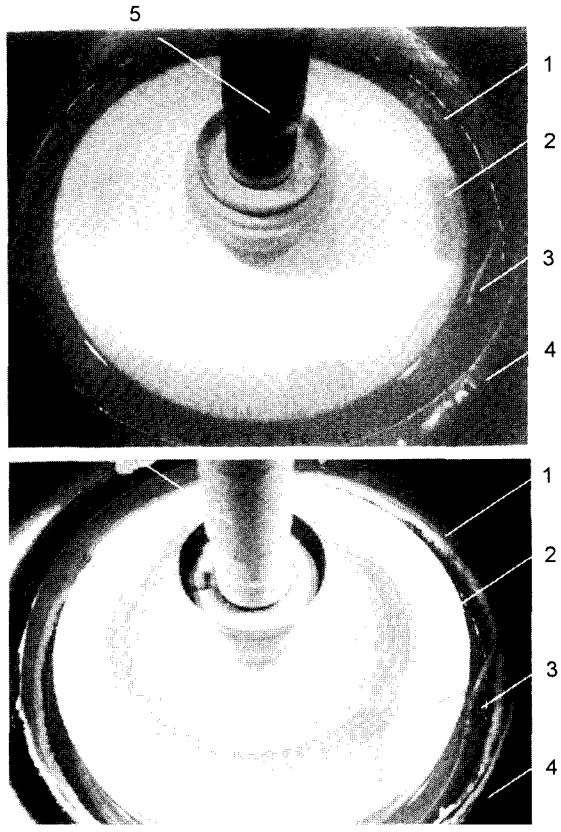

Fig. 11. Top butt view of a NaI (Tl) single crystal of 520 mm dia. after diameter growth duration 70 h (upper photo) and 60 h (lower photo). The photos have been taken under external ippumination. 1- the free melt surface; 2- the crystal butt; 3- the melt level sensor probe; 4-circular peripheral vessel of the crucible; 5- the crystal holder rod.

Fig. 11, presented are two examples of crystal growing at different radial speeds where the gas phase deposit layer density difference is seen. The photos evidence different deposit layer structures. On the crystal grown at higher growth speed, steps at its surface are seen (formed by the pulse pulling) where at lower growth speed, the steps are almost unobservable, thus evidencing a thicker deposit layer.

The bottom heater temperature (Fig. 12, curve 1) for the crystal shown in the lower photo of Fig. 11 was 23°C higher than for the compared one (Fig. 12, curve 2). (It is to note that the above-mentioned photo was made when the crystal cylinder attained already some height). It is to note also that, when the crystal grows in length, the melt gas phase is deposited mainly at the side cylindrical surface. The radial crystal growth speed providing the least number of structure defects and eliminating a situation similar to that shown in Fig. 9 amounts 5 to 7 mm/h. The minimum permissible value is 2.5 mm/h while the crystal growth up to the final constant diameter at lower speeds may indeed result in the

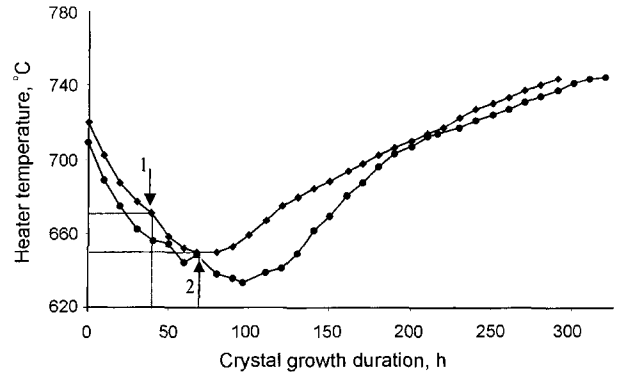

Fig. 12. The bottom heater temperature variation in growing of large NaI (Tl) crystals of 440 mm dia. at the radial growth speed of 4.4 mm/h (curve 1) and 2.5 mm/h (curve 2). The arrows point the moment when radial growing is over and the longitudinal one is started.

structure defects described above.

2.6. *Temperature fluctuations and CF shape changes*

Under random temperature decrease at a rate exceeding 0.5°C/min, the CF decoration can occur in the crystal, as is shown in Fig. 13. Temperature fluctuations of heaters and thus of the melt are inherent in any control systems. Therefore, the CF shape may also fluctuate. In fact, this was revealed when growing silicon crystals [8, 9], KCl ones [10] as well as NaI (Tl) and CsI (Tl).

Figure 14 presents two modes of CF shape fluctua-

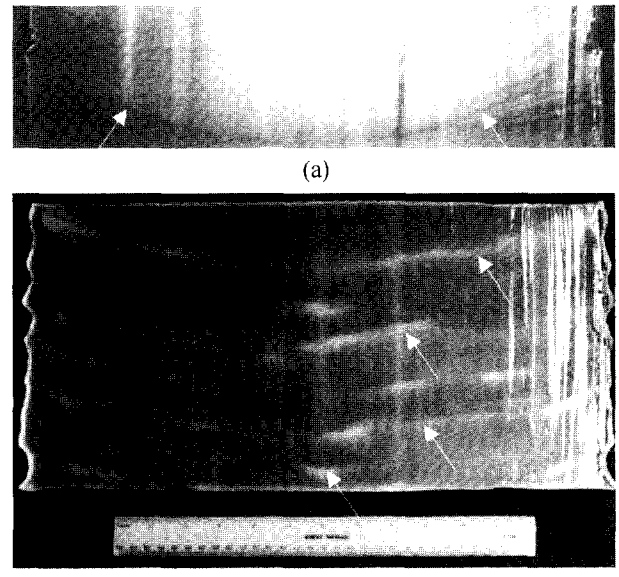

(a)

(b)

Fig. 13. Decoration (shown by arrow) of the CF shape due to temperature fluctuations of the bottom heater only (a) and of both heaters (b) in growing of NaI (Tl) single crystals of 450 mm dia.

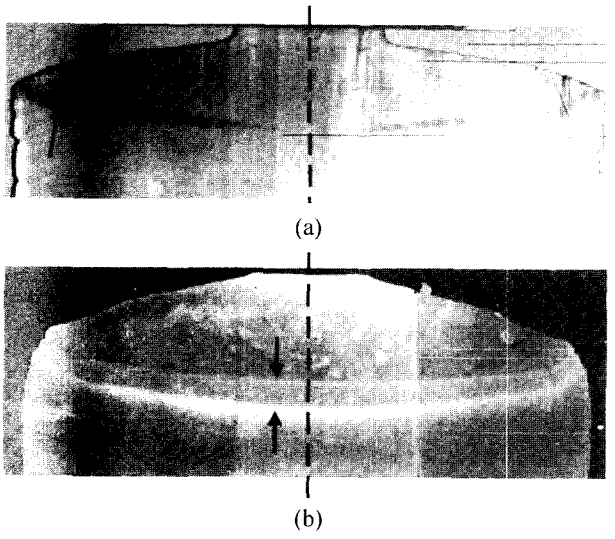

(a)

(b)

Fig. 14. CF shape variations in 520 mm dia. crystals due to heater temperature fluctuations: elevation of the bottom heater temperature accompanied by decrease of the side one (a) and vice versa (b). The upper arrow points the variation start, the lower one, the situation 4 (a) and 6 h (b) later, respectively.

tions under intentional change of the heater temperature in both directions. It is seen from the Figures that the temperature redistribution (T_{bot} elevation and T_{side} lowering) results in the predominated growth of the crystal periphery and a substantial stop of the growth in the CF center (Fig. 14a) and vice versa (Fig. 14b). As the heater temperature fluctuations become weaker, fluctuations of the interface or its local areas become smaller, respectively. Basing on experimental data, the heater temperature fluctuations, either controlled or random ones, occurring at a rate no more than 0.2°C/min are admissible from the standpoint of the crystal optical quality.

In this connection, it is of extreme importance to realize in practice the cascade scheme of temperature control that provides the heater temperature stabilization at maximum deviations no more than 0.3°C and the crystal diameter regulation based on the melt level lowering data [11].

From the standpoint of the automated system for the crystal diameter regulation, any CF shape may be suitable except for it should not be too flat; otherwise, the melt can tear off partially or completely from the CF surface at the crystal pulsed pulling.

2.7. *Activator distribution over large single crystal volume*

The impurity component distribution in crystals grown under melt feeding is defined, at the one hand, by the system properties and, at another one, by the growing conditions. For example, in conservative systems, approximated as flat CF and efficient mixing in liquid phase, two modes of impurity segregation can be distinguished depending on the process stage. At the steady stage, when the crystal diameter and the melt volume are constant, the impurity distribution in the crystal is defined by regularities known for zone crystallization.

The specific features of the system under study are described in detail in [9]. Here, only main relations will be presented.

The mass transfer due to evaporation can be reduced to one stage only, the mass transfer across the melt-gas phase interface described in the simplest case by Nernst equation

$$w = \frac{dn}{dt} = K_{LG} \cdot F(t)[C_L^0 - C_L(t)], \qquad (1)$$

where w is the impurity evaporation rate; dn, the impurity mass crossing the time-variable surface F(t) of the interface during the time dt; K_{LG}, coefficient characterizing the substance transport rate across the interface; $C_L(t)$, the real concentration of volatile impurity in the liquid; C_L^0, a quantity (constant for the specific system) presenting the hypothetical impurity concentration in the melt being in equilibrium with gas phase at temperature T_w (the impurity vapor pressure $P(T_w, C_L^0)$).

Taking into account the specific properties of system being considered and assuming the perfect melt mixing, we can write for the impurity mass transfer therein:

$$j = \frac{dn}{dt \cdot dF(t)} = K_{LG}[A - C_L(t)], \qquad (2)$$

where j is the specific impurity evaporation rate per unit phase interface area in unit time; A- a constant (in the ideal solution approximation, it is equal to the impurity vapor pressure above the solution, $P(T_w, C_L^0)$, divided by its partial vapor pressure, $P(T_w)$, at the same temperature).

In the case of crystal growth from a constant liquid phase volume under melt feeding, the equation (2) can be shown to be reduced to j = const, thus, it becomes possible to calculate separately the parameters of mass transfer due to evaporation and of that due to crystallization.

The methodology of that separate calculation is based on that the crystal growth processes on a seed from a limited melt volume under feeding (being an analog of zone crystallization) are performed in three different stages, namely, transitional, steady, and final normal crystallization ones. At the steady stage, the crystallization occurs from a constant volume liquid with constant impurity

concentration therein equal to C_0/k, thus defining a uniform impurity distribution along the crystal being grown. At the growing on a seed, this means that the crystallization mass rate is constant and equal to the feeding one, the crystal diameter and the melt surface area are constant.

This fact allows the following conclusions to be drawn. If, at the known and constant distribution coefficient k_0 and the feed composition C_f, the impurity concentration in the crystal at the steady crystallization stage is C_s, then the impurity fraction in the melt should be $C_L^s = C_s/k$. Thus, the impurity fraction in the feed (C_0) related to the crystallization process can be defined as $C_0 = kC_L^s = C_s$. It follows that the remaining impurity fraction contained in the feed (C_g) defined as $C_f C_s$ passes through the melt in transit and evaporates (thus, it is related only to the mass transfer from the melt). This fraction may be said to be introduced into the melt only for compensation of its entrainment from the melt to cold walls and to have no relation to the crystallization process (at least at the steady stage). Accordingly, the evaporation rate expression takes the form:

$$j = \text{const} \tag{3}$$

and it characterizes the steady-state mass transfer process.

In other words, the impurity mass transfer at the steady stage of zone crystallization can be considered as two separate processes conditionally independent of each other, namely, the impurity mass transfer along the «*feed-melt-crystal*» path and the impurity transit along the «*feed-melt-gas phase-cool furnace walls*» one. Only the corresponding impurity fraction- C_s and C_g, respectively, is involved in each process, their sum defines the total impurity concentration in the feed material, $C_f = C_s + C_g$.

Since the impurity concentration in the melt at the steady process stage is constant ($C_L = C_s/k_0 = \text{const}$), it follows from the impurity mass flow balance that the mass rate of the impurity evaporation is

$$w_g = (C_f - C_S) \cdot S_S \cdot \rho_S \cdot v_p \tag{4}$$

Accordingly, the specific evaporation rate j can be defined as:

$$j = \frac{w_g}{F} = \frac{(C_f - C_S) \cdot S_S \cdot \rho_S \cdot v_p}{S_L - S_S} \tag{5}$$

or

$$j = \frac{(C_f - C_S) \cdot d_S^2 \cdot \rho_S \cdot v_p}{D^2 - d_S^2} \tag{6}$$

The expression (6) defines interconnections between the crystallization rate, the feed rate and composition, the growing crystal diameter and composition. Accordingly, all these quantities take the status of controlling (or controlled) parameters in crystal crowing by pulling on seed under melt feeding by the substance to be crystallized and can be used to control the crystal composition and the crystallization process as a whole.

If it is just the initial charge mass providing the required crystal composition that is selected as the controlling parameter (C_s being the controlled one), it can be determined using the expression

$$n_f = \rho_L \cdot V_L \cdot \left[\frac{j}{\rho_S \cdot v_p} \cdot \left(\frac{D^2}{d_S^2} - 1 \right) + C_S/k_0 \right], \tag{7}$$

where n_f is the initial impurity charge mass; V_L, the melt volume in the crucible at the steady process stage determined at the constant crystal diameter. Since, however, the impurity distribution coefficient in CsI(Tl) and NaI(Tl) systems is 0.18 and 0.2, respectively, the further feed composition required to obtain homogeneous crystal composition can be determined using the above relations.

In the case when the activator impurity has a higher vapor pressure than the matrix, the crystal diameter rise step can be performed using non-activated raw material while the activator introduction into the melt starts as the preset crystal diameter is attained; the preset activator concentration is attained at the cylindrical part length about 15 mm. This is the case when CsI (Tl) or NaI (Tl) crystals are grown. At 750°C, the activator (TlI) vapor pressure is more than 300 times higher than that of NaI (234 and 0.74 Torr, respectively) and more than 100 times higher than that of CsI (234 and 2.11 Torr, respectively).

The uniform activator distribution over the crystal volume is provided to within ±5 % by the absence of the concentration gradient over the ingot length (except for the initial activator introduction step), by only slight CF fluctuations and by the activator charging to changeable hoppers according to calculated schedule under account for specific growth process parameters.

When single crystals with low k values, e.g., CsI (Na), the activator is introduced into melt at the initial stage, being added directly into raw salt. When such crystals are grown at the d/D ratio of 0.83, the activator concentration increases along the ingot due to a monotonous increase of the crystallization front and corresponding volume diminution of melted zone.

To attain the homogeneous activator distribution, $C_s(l)$, in CsI (Na) crystals, the inverse problem is solved: the

melt volume increase is programmed basing on $C_s(l)$ changes. However, if it is not necessary to provide the maximum crystal diameter d_s (for a specific crucible size), then the parameter d_s that define in essence the CF area can be reduced according to the known CF dependence on the crystal diameter. This statement was confirmed at the d_s/D ration value of 0.74 corresponding to the crystal diameter 13 % smaller than the limiting one. The CF in such crystal has a sag no more than 20 mm (while being of 60 to 70 mm at the limiting crystal diameter).

3. Conclusions

To obtain reproducible results as to the growth process stability when growing crystals above 500 mm in diameter from a crucible at the constant melt level, the following conditions are found to be met:

1) The permissible values of the crucible and crystal rotation speed are to be within ranges of 0.8 to 1.5 and 1 to 2 min^{-1}, respectively (the crucible and crystal being rotated in the same direction).

2) As the crystal-to-crucible diameter ratio increases from 0.5 to 0.83, the formed crystallization front convex toward the melt changes only its curvature radius (increasing), while at higher ratios, the isothermal surface profile changes dramatically. The $d/D = 0.83$ is the limiting value.

3) The curvature of crystallization front convex toward the melt depends directly on the inhomogeneities of radial heat flow from the bottom heater to the crucible (the heat flow decrease from periphery to center).

4) The minimum position in the bottom heater temperature variation curve depends directly on the crystal radial growth speed that defines the transmittance of the crystal surface to its intrinsic IR radiation. The shorter is the ingot diameter growing time up to constant value, the higher is the minimum temperature and the earlier is its position at the time scale (at the crystal length axis).

5) As the crystal diameter increases, the crystallization front position relative to the melt free surface shifts towards the crucible bottom. If the crystallization front immersion depth into the melt is at least 10 mm, it is stable (at the crystal growth speed of 2 to 4 mm/h) both from the standpoint of bubble displacement and the activator distribution over the crystal volume and against external factors consisting mainly in the control-induced and spontaneous melt temperature fluctuations. If the immersion depth is less than 10 mm, the crystallization front is the origin of structure defects and a runoff for foreign impurities. At «negative» immersion, the melt lifted by the crystallization front can be torn off from the crystal resulting in formation of continuous or local voids of different size at the phase interface.

6) In the production of optical quality crystals, controlled or random heater temperature fluctuations are admissible when their rate does not exceed 0.2°C/min.

7) The uniform activator distribution over the crystal volume is provided to within ± 5 % by calculation algorithms constructed basing on the presented analytical expressions and taking into account the volatile component transit, the melt volume change and the specific parameters of the growth process.

References

[1] L.G. Eidelman, V.I. Goriltsky, V.A. Nemenov, V.G. Protsenko and A.V. Radkevich, "Automated growing of large single crystals controlled by melt level sensor", Crystal. Res. and Technol. 20(2) (1985) 167.

[2] L.G. Eidelman, V.I. Goriltsky, V.G. Protsenko, A.V. Radkevich and V.V. Trofimenko, "Automated pulling from the melt - an effective method of growing large alkali halide single crystals for optical and scintillation applications", J. Cryst. Growth. 128 (1993) 1059.

[3] V.I. Goriltsky, L.G. Eidelman, A.N. Panova and K.V. Shakhova *et al.*, "New scintillation material-CsI(CO_3)", Nucl. Tracs Radia. Meas. 31(1) (1993) 111.

[4] K.V. Shakhova, A.N. Panova and V.I. Goriletsky *et al.*, "Luminescent and scintillation properties of CsI-CsBr(Na) crystals", J. Radiation Measurements. 33 (2001) 769.

[5] V.I. Goriletsky and N.N. Smirnov, "The specifics of crystal growing in nonconsevative systems", J. Cryst. Growth 218 (2000) 125.

[6] S.K. Bondarenko, V.I. Goriletsky and V.S. Susdal, "Production of large CsI(Tl) single crystals grown by semi-continuous automated method", Functional Materials 6(2) (1999) 380.

[7] V.I. Goriletsky and S.K. Bondarenko, "Production of preset quality large NaI(Tl) single crystals for detectors used medical instrument bulding", J. Mat. Sci. & Ing. A. 288(2) (2000) 196.

[8] V.S. Suzdal, Yu. M. Epifanov, V.N. Zvyagiontsev, L.I. Gerasimchuk., I.L. Tavrovsky, N.I. Strelnikov and M.P. Artemenko, "Rasvitie cictem upravlenia processamy poluhenia krupnogabaritnyh monokristallov iz rasplava", Radioelectronika i informatika 4(17) (2001) 91.

[9] N.N. Smirnov, V.I. Goriletsky and S.K. Bondarenko, "Crystallization processes control on growing large dimension crystals out of the melt", Functional Materials 7(4) (2000) 41.